Arabian Journal of Chemistry (2022) **15**, 104100

King Saud University

Arabian Journal of Chemistry

www.ksu.edu.sa
www.sciencedirect.com

ORIGINAL ARTICLE

Phenylpropenol ester and sesquiterpenoids with antimetastatic activities from the whole plants of *Chloranthus japonicus*

Rong Lin [a,1], Ronghao Sun [a,1], Ting Xiao [a,1], Suyu Pei [a], Qiang Zhang [b], Yexin Cheng [a], Xiaowei Guo [a], Zhongyi Yang [c], Xiaoting Gu [a], Fubo Zhang [d,*], Chunfeng Xie [a,*], Cheng Yang [a,*]

[a] *State Key Laboratory of Medicinal Chemical Biology, College of Pharmacy and Tianjin Key Laboratory of Molecular Drug Research, Nankai University, Haihe Education Park, 38 Tongyan Road, Tianjin 300353, People's Republic of China*
[b] *Shaanxi Key Laboratory of Natural Products & Chemical Biology, College of Chemistry & Pharmacy, Northwest A&F University, Yangling 712100, People's Republic of China*
[c] *School of Pharmacy, Shandong University of Traditional Chinese Medicine, 4655 University Road, University Science Park, Changqing District, Jinan, Shandong 250355, People's Republic of China*
[d] *Organ Transplantation Center, Tianjin First Central Hospital, No.24 Fukang Road, Nankai District, 300192 Tianjin, People's Republic of China*

Received 14 April 2022; accepted 2 July 2022
Available online 6 July 2022

KEYWORDS

Chloranthus japonicus;
Chloranthaceae;
Lindenane sesquiterpenes;
Antimetastatic effect;
Human hepatocarcinoma;
Epithelial-mesenchymal transition

Abstract One new phenylpropenol ester (**1**) and three new lindenane sesquiterpenes (**2**–**4**) were isolated from the whole plant of *Chloranthus japonicus* together with three known lindenane derivatives (**5**–**7**). Their structures were determined based on detailed spectroscopic and electronic circular dichroism computational analyses. Compound **4** showed moderate efficacy in inhibiting cell migration, invasion, and vasculogenic mimicry (VM) in human of hepatocarcinoma (HCC) HepG2 cells. Furthermore, compound **4** could alter the expression of the proteins Vimentin, N-cadherin, Snail1 and E-cadherin by down-regulating the expression of Twist1, which indicated that its antimetastatic effect was associated with restraining the epithelial-mesenchymal transition (EMT) in HepG2 cells.

[1] These authors contributed equally.
[*] Corresponding authors.
E-mail addresses: 251809@163.com (F. Zhang), xiechunfeng@nankai.edu.cn (C. Xie), cheng.yang@nankai.edu.cn (C. Yang).
Peer review under responsibility of King Saud University.

Production and hosting by Elsevier

https://doi.org/10.1016/j.arabjc.2022.104100
1878-5352

1. Introduction

Primary liver cancer ranks sixth in morbidity and second in mortality in the world. Hepatocellular carcinoma is the most common primary liver cancer, accounting for more than 85% of liver cancer cases (Lee and Cheung, 2019). Patients at the early stage of HCC often need liver transplantation and surgical resection. After surgery, the 5-year recurrence rate is still higher than 70% (Tella et al., 2022). Sorafenib and lovatinib are commonly used as targeted drugs for advanced HCC, but their clinical efficacy is not perfect; they can prolong the survival time by only approximately three months (Kudo et al., 2018). Although there are many other drugs for HCC on the market, the treatment results of HCC are unsatisfactory, and the 5-year survival rate of HCC is no more than 18% (Bruix et al., 2017, Abou-Alfa et al., 2018). More effective treatment strategies and drugs with higher efficacy remain urgent.

HCC has a strong vascular invasion and metastasis ability and is one of the most common invasive malignant tumors. Its high recurrence rate is mainly due to the spread of intrahepatic metastasis (Braun et al., 2022). There is increasing evidence that epithelial-mesenchymal transformation (EMT) is a complex process that is closely related to the metastasis of HCC cells. EMT is the process that epithelial cells lose the apical-basal polarity and cell–cell adhesion, and transit to invasive mesenchymal cells. Usually, E-cadherin acts as the marker protein of epithelial phenotype, while Vimentin, Snail1 and N-cadherin are the marker proteins of mesenchymal phenotype. The changes in gene expression during EMT lead to numerous phenotypic changes, such as cell morphological changes, loss of adhesion and gain of stem cell-like features (Huang et al., 2022). The existence of VM in HCC is considered to be closely related to poor prognosis, high invasion and metastasis and high recurrence rate of HCC. Previous studies have shown that EMT is a necessary factor in the formation of VM. From this point of view, EMT is a key factor in HCC invasion and metastasis, and the inhibition of the EMT process will effectively prevent the invasion and metastasis of tumor cells (Zheng et al., 2021).

Chloranthus japonicus Sieb. is a plant species of Chloranthaceae and is distributed mainly in China. Its whole plants, namely, Yin-xian-cao, have been used to treat various diseases, such as cold cough, carbuncles and furuncles, in traditional Chinese medicine (Nanjing University of Chinese Medicine, 2006). Sesquiterpenoid derivatives, especially lindenane sesquiterpenes, are rich in *C. japonicus* with multiple bioactivities, such as anti-HIV, cytotoxic, and anti-inflammatory activities (Kim et al., 2016, Yan et al., 2016, Zhao et al., 2016, Zhuo et al., 2017).

In our ongoing studies on bioactive ingredients from *Chloranthus* plants (Xie et al., 2015), the chemical constituents of *C. japonicus* have been studied. Seven compounds, including one new phenylpropenol ester and three new sesquiterpenes, have been isolated from *C. japonicus*. The separation, structural elucidation, and evaluation of their antimetastatic effects against human hepatocarcinoma HepG2 cells for all isolates from *C. japonicus* are presented in this paper.

2. Materials and methods

2.1. General experimental procedures

The instruments and materials for the isolation and structural identification were the same as those in our previous report (Ding et al., 2020).

2.2. Plant material, extraction and isolation, and ECD calculations

The details on the plant material, extraction and isolation, and the calculations for the ECD spectra are provided in the Supporting Information.

2.2.1. 2,3,4-Trimethoxycinnamyl senecioate (*1*)

Yellow oil; IR (KBr) ν_{max} 2930, 1717, 1650, 1583, 1506, 1457, 1419, 1380, 1332, 1228, 1184, 1144, 1008, 968, 849 cm^{-1}; ^1H NMR (400 MHz, $CDCl_3$) and ^{13}C NMR (100 MHz, $CDCl_3$) data, see Tables 1 and 2; HR-ESIMS *m/z* 307.1540 $[M + H]^+$ (calcd for $C_{17}H_{23}O_5$ 307.1545).

2.2.2. Chlorajapolide J (*2*)

Yellow oil;[α] − 21.9 (*c* 0.24, CH_2Cl_2); ECD (CH_3CN) λ_{max} (Δε) 212 (−2.43), 241 (1.55) nm; IR (KBr) ν_{max} 2954, 2927, 1731, 1436, 1376, 1312, 1272, 1224, 1174, 1110, 1083, 1047, 1019, 962, 938, 856 cm^{-1}; ^1H NMR (400 MHz, $CDCl_3$) and ^{13}C NMR (100 MHz, $CDCl_3$) data, see Tables 1 and 2; HR-ESIMS *m/z* 351.1441 $[M + H]^+$ (calcd for $C_{18}H_{23}O_7$ 351.1444).

2.2.3. Chlorajapolide K (*3*)

Colorless oil; [α] − 16.0 (*c* 0.19, CH_2Cl_2); ECD (CH_3CN) λ_{max} (Δε) 216 (−2.82), 234 (0.59), 255 (−2.28) nm; IR (KBr) ν_{max} 3077, 2926, 2854, 2359, 1774, 1743, 1661, 1541, 1456, 1371, 1263, 1226, 1162, 1136, 1083, 1045, 1019, 970, 924, 896, 748 cm^{-1}; ^1H NMR (400 MHz, $CDCl_3$) and ^{13}C NMR (100 MHz, $CDCl_3$) data, see Tables 1 and 2; HR-ESIMS *m/z* 335.1490 $[M + H]^+$ (calcd for $C_{18}H_{23}O_6$ 335.1495).

2.2.4. Chlorajapolide L (*4*)

White amorphous powder; [α] − 258.9 (*c* 0.14, CH_2Cl_2); ECD (CH_3CN) λ_{max} (Δε) 213 (12.47), 246 (4.57) nm; IR (KBr) ν_{max} 3079, 2936, 2360, 1771, 1664, 1456, 1375, 1323, 1239, 1223, 1196, 1146, 1108, 1087, 1056, 1035, 1014, 986, 941, 921, 887, 794, 762 cm^{-1}; ^1H NMR (400 MHz, $CDCl_3$) and ^{13}C NMR (100 MHz, $CDCl_3$) data, see Tables 1 and 2; HR-ESIMS *m/z* 335.1490 $[M + H]^+$ (calcd for $C_{18}H_{23}O_6$ 335.1495).

2.3. Chemicals and reagents for biological evaluation

Antibodies to GAPDH, E-cadherin, Vimentin, Snail, N-cadherin and Twist1 were purchased from Affinity (USA). Goat pAb to Rb IgG(HRP) was purchased from ImmunoWay (China). Matrigel and transwell chambers were purchased from BD Biosciences (San Jose, CA, USA). All cell culture reagents were obtained from Hyclone Co. (Suzhou, China).

2.4. Cell lines and culture

Human liver cancer cells (HepG2, ATCC) and human gastric cancer cell lines (HGC-27, ATCC) were stored in DMEM (KeyGEN BioTECH, China) with 10% fetal bovine serum (FBS, ExCell Bio, China) and 1% antibiotics (penicillin streptomycin, Gibco). Human cervical cancer cells (Hela, ATCC) and human ovarian cancer cells (SKOV3, ATCC) were stored in RPMI 1640 (KeyGEN BioTECH, China). All cells were stored in an incubator at 37 °C with 5% CO_2 humidification.

2.5. MTT assay

MTT assay was used to detect the cell survival rate after different compound treatments. HepG2 cells, Hela cells and HGC-27 cells were cultured at a concentration of 5×10^4 cells/mL in a 96-well plate for 24 h, and different compounds with concen-

Table 1 ^{1}H NMR Data for Compounds **1**–**4** ($CDCl_3$, 400 MHz, δ in ppm, J in Hz).

Position	**1**	**2**	**3**	**4**
1	6.62 s	1.68 *m*	2.15 *m*	1.96 *m*
2α		0.74 *m*	0.71 *m*	0.98 *m*
2β		1.48 *m*	0.84 *m*	0.79 *m*
3		1.56 *m*	1.97 *m*	1.94 *m*
4				
5	6.62 s	3.02 d (4.6)	3.52 *m*	3.37 d (12.4)
6		5.62 d (4.6)	5.74 d (10.7)	5.40 d (12.4)
7	6.58 d (16.1)			
8	6.23 dt (6.3, 16.1)			
9	4.74 d (6.3)	9.50 s	3.84 d (6.8)	4.03 s
10				
11				
12				
13		2.18 s	2.03 s	1.92 s
14		1.22 s	0.58 s	0.96 s
15		1.58 s	4.70 br s, 5.02 br s	4.85 br s, 5.07 br s
1′		2.10 s	2.09 s	2.21 s
2′	5.73 s			
3′				
4′	2.19 s			
5′	1.91 s			
1″	3.87 s	3.77 s	3.27 s	3.28 s
2″	3.85 s			
3″	3.87 s			

Table 2 ^{13}C NMR Data for Compounds **1**–**4** ($CDCl_3$, 100 MHz, δ in ppm).

Position	**1**	**2**	**3**	**4**
1	103.7	25.1	23.1	24.1
2	153.3	5.1	15.9	16.4
3	138.1	27.3	23.5	23.3
4	153.3	91.4	149.3	147.8
5	103.7	47.4	56.5	58.9
6	132.1	66.5	63.2	69.5
7	133.8	127.4	150.9	153.5
8	123.3	165.2	105.8	109.7
9	64.1	200.8	79.2	74.7
10		58.1	43.8	42.8
11		140.9	133.9	126.3
12		169.3	170.4	171.0
13		16.6	9.4	8.5
14		15.2	20.8	17.3
15		31.9	107.5	109.1
1′	166.4	21.2	20.7	20.6
2′	115.7	169.2	169.9	170.5
3′	157.4			
4′	20.3			
5′	27.5			
1″	56.1	52.8	50.1	50.8
2″	60.9			
3″	56.1			

tration of 50 μM were added after cell adherence. After 48 h of incubation, 20 μL MTT solution was added to each well and incubated at 37 °C for 4 h. The absorbance of the solution was quantified at 570 nm wavelength by using a microplate reader (Mul-tiskan™FC, Thermo Scientific, Waltham, MA, USA).

2.6. Wound healing assay

HepG2 cells were grown on 24-well plates to 100% confluence. The 100 μm wounds were scratched using sterile pipette tips. Then HepG2 cells were cultured with compounds **1**–**7**

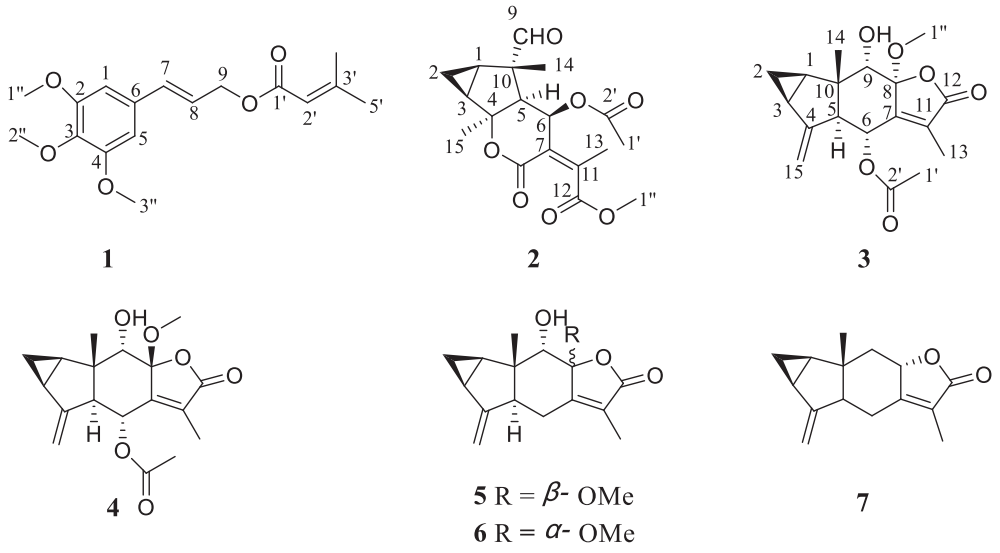

Fig. 1 Chemical structures of compounds **1**–**7**.

(50 μM). The scratch was observed at 0, 24, 48 h by a light microscope (Nikon, Japan). After that, the drug with the strongest inhibition of cell migration was selected and the concentration gradient was set for the wound healing assay again. Subsequently, compound **4** was selected for follow-up experiments. Compound **4** (30, 60 and 120 μM) were added to cells cultured for 0, 24, 48 h. The images of the cells were acquired with a light microscope (Nikon, Japan).

2.7. Three-dimensional culture assay

HepG2 cells were seeded in 96-well culture plates prepared with Matrigel (BD Biosciences). The cells were co-incubated with various concentrations of compound **4** (30, 60, and 120 μM). After incubation for 24 h, cell images were captured using the light microscope (Nikon, Japan).

2.8. Transwell assays

HepG2 cells were seeded onto a chamber coated with matrigel (BD, USA) and inserted into the wells of a 24-well plate. The 24-well plate were filled with FBS-containing complete medium. Different concentrations of compound **4** were added into the chamber, after 24 h HepG2 cells migrating to the lower surface were fixed and stained.

2.9. Western blot analysis

Proteins were extracted from the HepG2 cells treated with different concentrations of compound **4** and analyzed through western blot analysis. Whole-cell lysates were analyzed with sodium dodecyl sulfate–polyacrylamide gel electrophoresis (SDS–PAGE), transferred to polyvinylidene fluoride (PVDF) membrane (Milan, Italy), then the membranes were blocked with 5% fat free milk. The membrane incubated at 4 ℃ overnight with monoclonal antibodies against GAPDH, E-cadherin, Vimentin, N- cadherin, Snail1 and Twist1. The membrane was further incubated with secondary antibodies (Affinity, 1:10000). Finally, the membrane was subjected to an electrophoresis gel imaging system (ChemiScope 6000, CLIX, Shanghai, China).

2.10. Statistical analysis

Statistical analyses were performed with GraphPad Prism 7.0. The significance differences between groups were calculated by student *t* test. Significant differences among multiple groups were detected by one-way ANOVA. $P < 0.05$ was considered as statistically significance.

3. Results and discussion

3.1. Structural elucidation

Chemical research on *C. japonicus* resulted in one new phenylpropenol ester (**1**), three new sesquiterpenes (**2**–**4**) and three known compounds (**5**–**7**) (Fig. 1). The known compounds were identified as 8-epimer-chlorajapolide F (**5**) (Zhang et al., 2012), chlorajapolide F (**6**) (Zhang et al., 2012), and shizukanolide (**7**) (Kawabata et al., 2014), respectively.

Compound **1** was obtained as a yellow oil. Its HR-ESIMS showed a $[M + H]^+$ peak at *m/z* 307.1540 and determined the molecular formula of $C_{17}H_{22}O_5$ (calcd for $C_{17}H_{23}O_5$ 307.1545). The carbonyl (1717 cm^{-1}) and double bond (1650 cm^{-1}) functional groups were found in the IR spectrum. The ^1H NMR spectrum (Table 1) showed the presence of three methoxy groups at δ_H 3.87 (s, 6H) and 3.85 (s, 3H), two methyl groups at δ_H 2.19 (s, 3H) and 1.91 (s, 3H), five olefinic methines at δ_H 6.62 (s, 1H*2), 6.58 (d, J = 16.1 Hz, 1H), 6.23 (dt, J = 6.3, 16.1 Hz, 1H) and 5.73 (s, 1H), and an oxygenated methylene at δ_H 4.74 (d, J = 6.3 Hz, 2H). The ^{13}C NMR data (Table 2) of **1** included 14 carbon signals. It was apparent that one senecioyl group (δ_C 166.4, 157.4, 115.7, 27.5, and 20.3) appeared in the NMR spectra (D'Ambrosio, et al., 2015). The remaining resonances comprised a symmetrical 1, 3, 4, 5-tetrasubstitution benzene at δ_C 153.3 (×2), 138.1, 132.1,

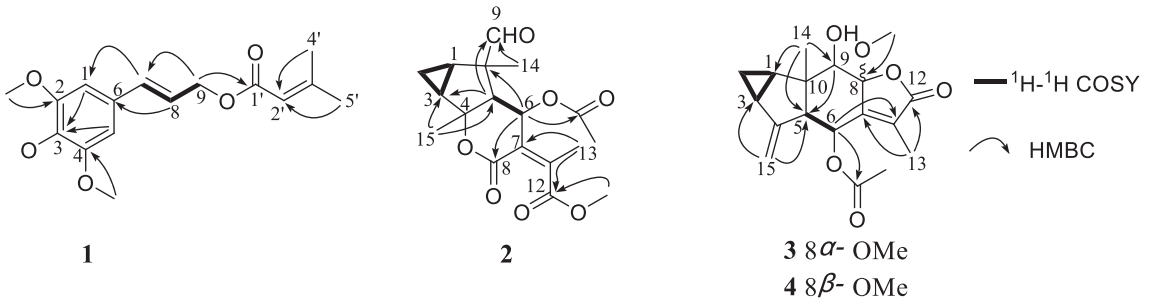

Fig. 2 Selected ^{1}H–^{1}H COSY and HMBC correlations of compounds **1**–**4**.

and 103.7 (×2), one oxygenated methylene at δ_C 64.1, two olefinic methines at δ_C 123.3 and 133.8, and three methoxy groups at δ_C 56.1 (×2) and 60.9. According to the spectroscopic data, compound **1** might be a phenylpropenol ester derivative (Fan et al., 2009). Detailed comparison with the known compound 3′,4′,5′-trimethoxy cinnamyl caproate revealed that the NMR data of **1** (Tables 1 and 2) resembled those of this compound (Sun, et al., 2016), except for a senecioyl group in **1** instead of a hexanoyl group attached to C-9 in 3′,4′,5′-trimethoxycinnamyl caproate, which was confirmed by the ^{1}H–^{1}H COSY correlations of H-7/H-8/H_2-9 and HMBC correlation from H-9 (δ_H 4.74) to C-1′ (δ_C 166.4) (Fig. 2). The configuration of the double bond $\Delta^{7,8}$ was established as *E* according to the coupling constant (J = 16.1 Hz). The structure of **1** was therefore elucidated as 2, 3, 4-trimethoxycinnamyl senecioate.

The molecular formula of compound **2** was deduced to be $C_{18}H_{22}O_7$ according to HR-ESIMS (*m*/*z* 351.1441 $[M + H]^+$, calcd for $C_{18}H_{23}O_7$ 351.1444). In the ^{1}H NMR spectrum, five methyl signals at δ_H 2.18 (s, 3H), 1.22 (s, 3H), 1.58 (s, 3H), 2.10 (s, 3H), and 3.77 (s, 3H), one oxygenated methine at δ_H 5.62 (d, J = 4.6 Hz, 1H), and one formyl proton at δ_H 9.50 (s, 1H) were observed (Table 1). The ^{13}C NMR spectrum exhibited eighteen carbon resonances (Table 2). It was obvious that an acetoxy group (δ_H 2.10 and δ_C 169.2, 21.2) and a methoxy (δ_H 3.77 and δ_C 52.8) group were present, which suggested **2** as a sesquiterpene with one acetoxy and one methoxy groups. The ^{13}C and ^{1}H NMR data of **2** demonstrated a resemblance with those of the known compound chloranerectuslactone V isolated from *C. erectus* (Thu Huong et al., 2014) except for an additional C-6 acetoxy group. This deduction was further verified by the HMBC correlation from H-6 (δ_H 5.62) to C-2′ (δ_C 169.2) as shown in Fig. 2. The relative configuration of **2** was established from the NOESY spectrum (Fig. 3). The cross-peaks of H_3-15/H-6, H_3-15/H-5, H-9/H-5, H-9/H-1, H-3/H-2α, and H-1/H-2α indicated that they adopted an α-orientation, while H_3-14 was assigned as *β*-oriented. Additionally, the NOESY correlation of H-6/H_3-13 suggested a *Z*-configuration of the $\Delta^{7,11}$ olefinic bond. The absolute configurations were assigned as 1*R*, 3*S*, 4*S*, 5*S*, 6*R*, and 10*S* using the calculated and experimental ECD comparison (Fig. 4). The structure of **2** was thus finally elucidated and named chlorajapolide J. Compound **2** represented a rare example of the rearranged 8,9-*seco*-lindenanes previously found in *Sarcandra glabra* (Chi et al., 2019), *Chloranthus erectus* (Thu Huong et al., 2014), *Lindera strychnifolia* (Kouno et al., 2001; Liu et al., 2013; Sumioka et al., 2011), *L. chunii* (Zhang et al., 2002), and *L. aggregata* (Gan et al., 2009).

Compound **3** was isolated as a colorless oil and assigned the molecular formula of $C_{18}H_{22}O_6$ deduced from the HR-ESIMS data. The ^{1}H NMR spectrum of **3** (Table 1) exhibited signals typical of the cyclopropane ring of lindenane sesquiterpenoids (Yan et al., 2013), including four upfield protons at δ_H 0.71 (1H, m, H-2b), 0.84 (1H, m, H-2a), 1.97 (1H, m, H-3), and 2.15 (1H, m, H-1). Additionally, two terminal olefinic protons at δ_H 5.02 (1H, br s, H-15a) and 4.70 (1H, br s, H-15b) implied that **3** bore a 4(15)-en-lindane skeleton. This induction was supported by the occurence of the ^{1}H–^{1}H COSY correlations of H-1, H_2-2 and H-3 and the correlations of H_2-15 to C-5 (δ_C 56.5) and C-3 (δ_C 23.5) in the HMBC spectrum (Fig. 2). The carbon signals at δ_C 169.9, 20.7, and 50.1 in the ^{13}C NMR spectrum (Table 2) together with the corresponding ^{1}H NMR data suggested the existence of an acetoxy and a methoxy groups. The ^{13}C and ^{1}H NMR spectroscopic data of **3** were comparable to those of 8-epimer-9-hydroxy-heterogorgiolide isolated from the same plant species (Zhang et al., 2012), apart from an additional acetoxy group. The significant down-field shift of C-6 revealed that the acetoxy group was attached at C-6 (δ_C 63.2,

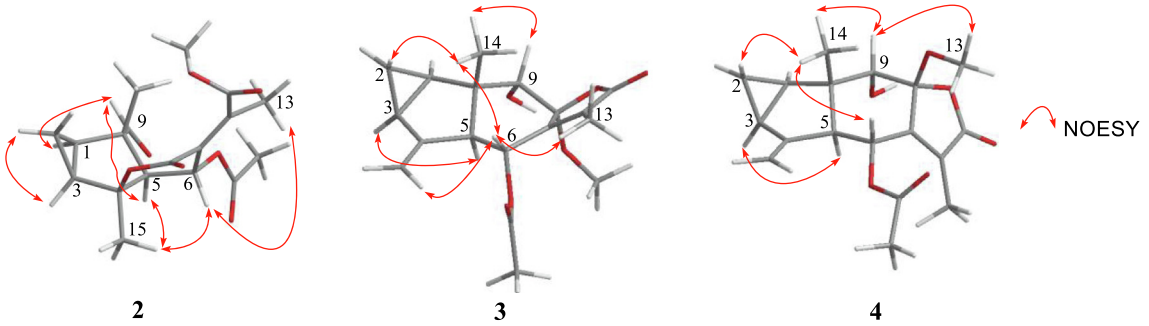

Fig. 3 Selected NOESY correlations of compounds **2**–**4**.

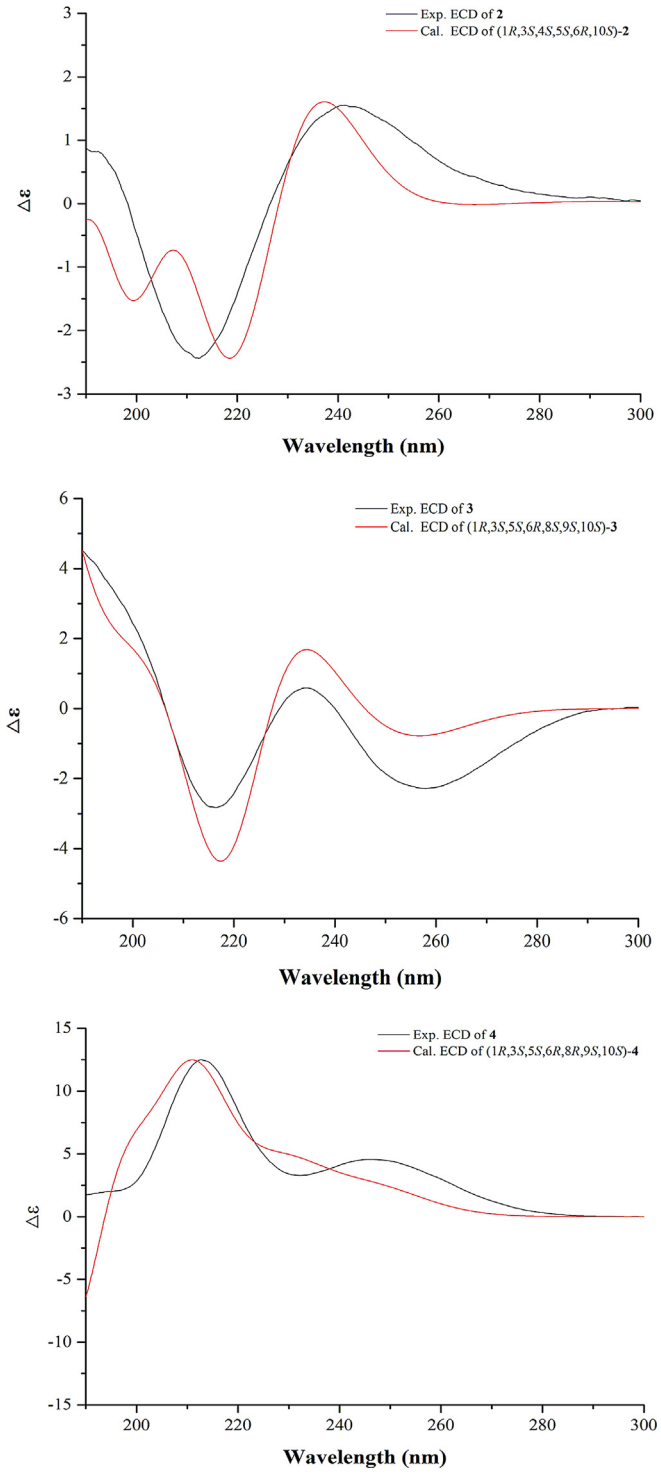

Fig. 4 Calculated and experimental ECD spectra of compounds **2**–**4.**

$\Delta\delta$ + 40.4), which was sustained through the correlation of δ_H 5.74 with δ_C 169.9 in the HMBC spectrum (Fig. 2). The relative configuration of **3** was elucidated through a NOESY experiment (Fig. 3). The correlations of H-6/H-15a, H_3-13, and H_3-14, H_3-14/H-9 and H-2β, H-2α/H-1 and H-3, H-5/8-OMe indicated that the cyclopropane ring and H_3-14 were β-oriented, and that H-5, 6-OAc, 8-OMe and 9-OH were α-oriented. The absolute configurations of (1*R*, 3*S*, 5*S*, 6*R*, 8*S*, 9*S*, 10*S*) were determined for **3** by ECD analysis (Fig. 4). The structure of **3** was thus elucidated and named chlorajapolide K.

Compound **4** was isolated as a white amorphous powder. Its molecular formula was determined to be $C_{18}H_{22}O_6$ according to the protonated molecular ion peak at *m*/*z* 335.1490 $[M + H]^+$ (calcd for $C_{18}H_{23}O_6$ 335.1495) and 1D NMR data. The ^1H and ^{13}C NMR spectroscopic data of **4** closely resem-

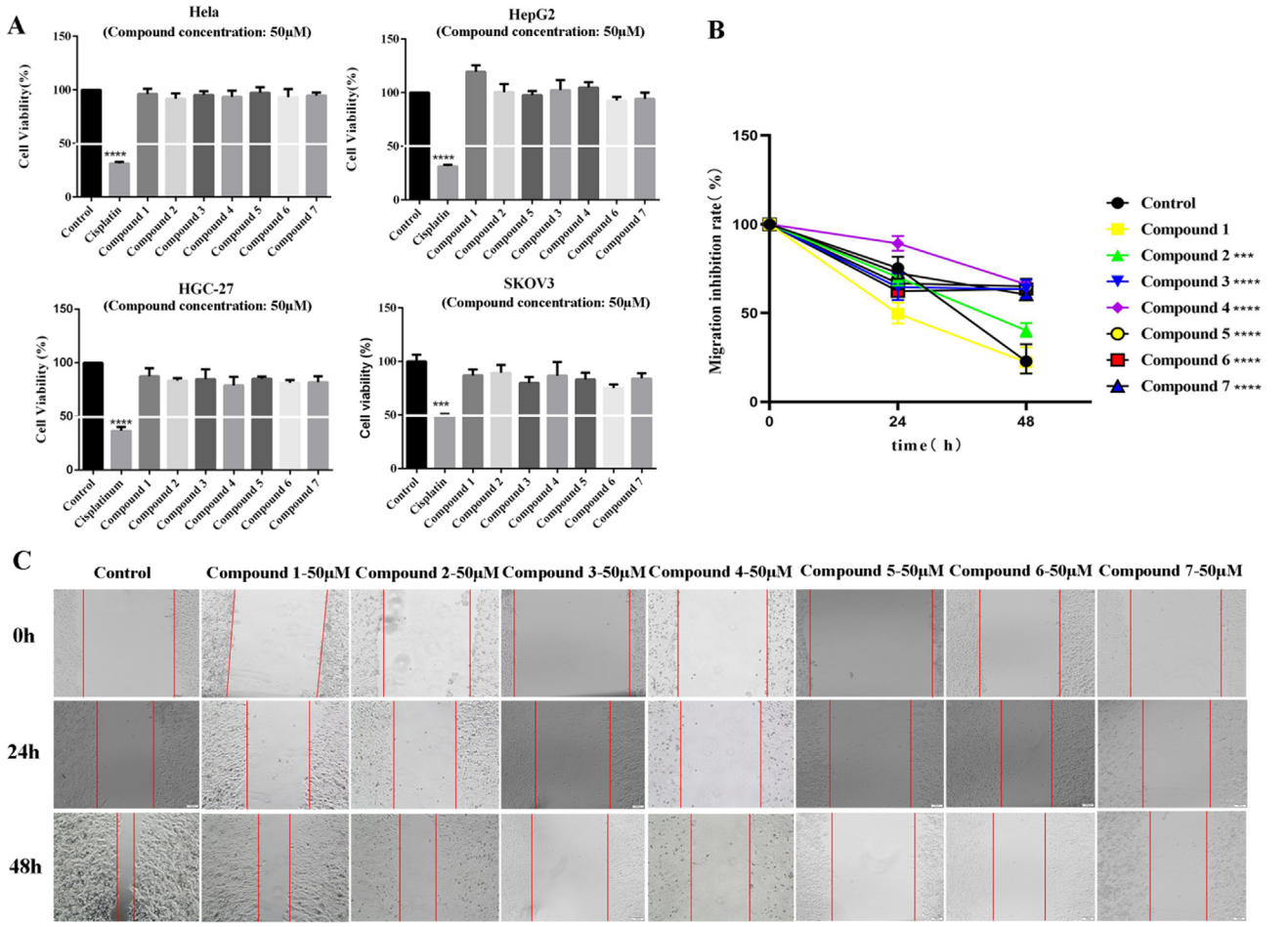

Fig. 5 Compound **4** can significantly inhibit the migration but not the cell viability of HepG2 cells *in vitro*. (A) Cell viability tests on Hela, HepG2, HGC-27 and SKOV3 cells showed that compounds **1**–**7** did not inhibit the activity of cancer cells at the concentration of 50 μM within 48 h. (B, C) Compounds **1**–**7** were added to HepG2 cells for wound healing assays. Compound **4** had the strongest migration inhibitory effect on HepG2 cells at a concentration of 50 μM. (Data are represented as the means ± SDs, n = 3. * $P < 0.05$, ** $P < 0.01$, *** $P < 0.001$, ****$P < 0.0001$.).

bled those of **3** with the exception of the down-field shifted C-6 (δ_C 69.5) and C-7 (δ_C 153.5) as well as the up-field shifted C-9 (δ_C 74.7) and C-11 (δ_C 126.3) (Table 2). This indicated that compound **4** bore a similar structure as **3** with a different stereochemistry. In the NOESY spectrum (Fig. 3), the correlations of 8-OMe/H-9, H_3-14, H3-14/H-2β, H-6, H-9, H-2α/H-3, and H-1 suggested that the cyclopropane ring, 8-OMe and H_3-14 were β-oriented, and that H-5, 6-OAc, and 9-OH were α-oriented. The absolute configuration was assigned as 1*R*, 3*S*, 5*S*, 6*R*, 8*R*, 9*S*, and 10*S* because of the similarity between the calculated and experimental ECD data (Fig. 4). Consequently, the structure of compound **4** was determined to be a C-8 epimeric isomer of **3** and named chlorajapolide L.

*3.2. Compound **4** can significantly inhibits the migration and invasion but not the cell viability of HepG2 cells in vitro*

Cell activity detect is a classical research method for evaluating the antitumor effect of compounds. To explore the antitumor activity of compounds **1**–**7**, we evaluated the inhibitory effects on the activity of liver cancer cells (HepG2), cervical cancer cells (Hela), stomach cancer cells (HGC-27) and ovarian cancer cells (SKOV3), which are common and high incidence tumor types, by the MTT method. Different cancer cells were treated with all compounds for 48 h. At a concentration of 50 μM, none of the isolates showed obvious antitumor activity on four cancer cells (Fig. 5A). The high migration and invasion ability of tumor cells is an important basis of tumor metastasis (Gundamaraju et al., 2022). HCC has a strong vascular invasion and metastasis ability and is one of the most common invasive malignant tumors. In order to further explore the inhibitory activity of all compounds on tumor cell migration, we evaluated the inhibitory effect of all compounds on HepG2 cells migration. HepG2 cells were treated with seven compounds with 50 μM for 48 h. The results of migration inhibit rate showed that compound **4** exhibited the most obvious inhibitory effect on cell migration (Fig. 5B, 5C), revealing that the C-8 configuration and the substituents at C-6 might have an important effect on the antimetastatic activities of lindenrane sesquiterpenoids. Besides, we also detected the inhibitory effect of compound **4** on four cancer cells migration. The results showed that HepG2 cells are the most sensitive to compound **4** (Fig. S38, Supporting Information).

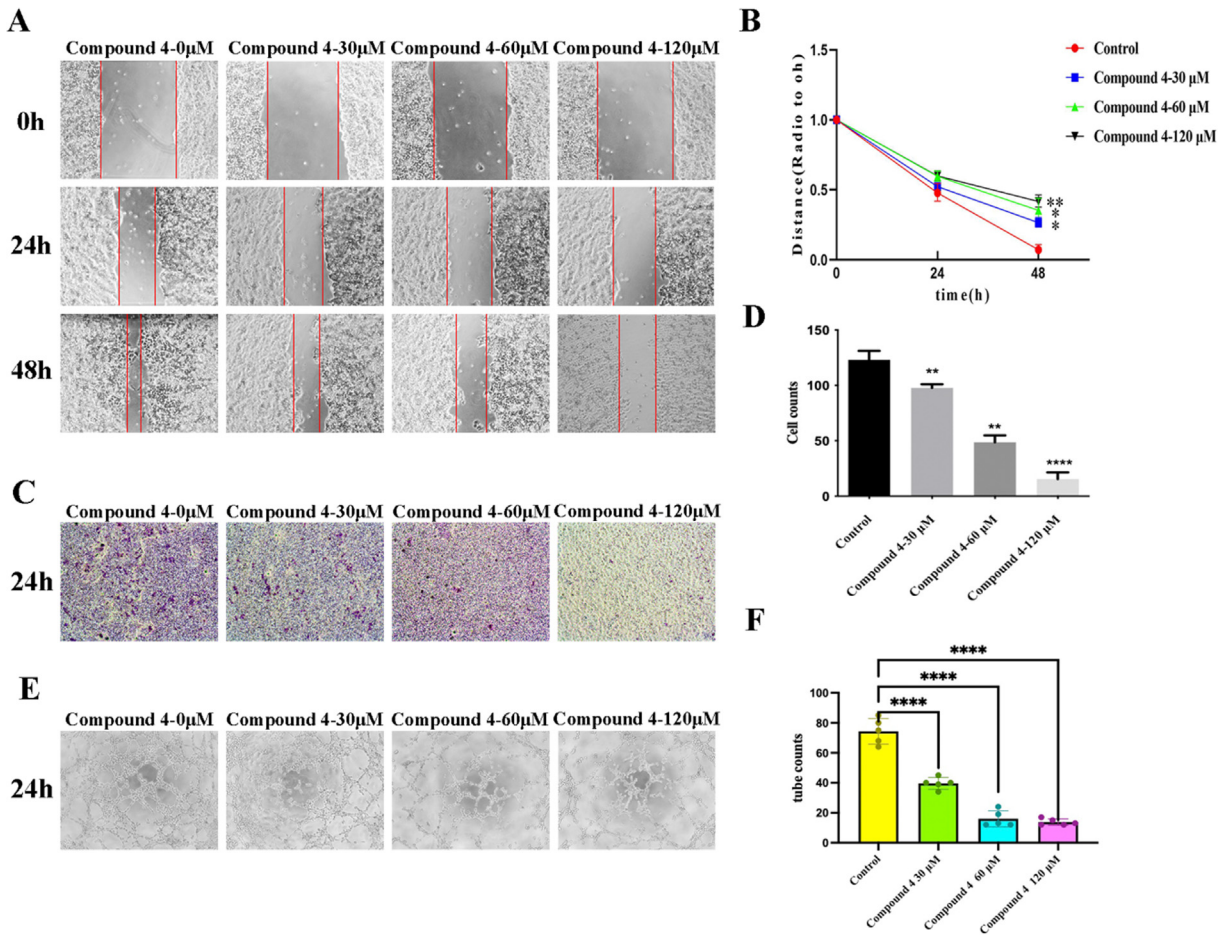

Fig. 6 Compound **4** inhibited the migration, invasion and tube formation of HepG2 cells *in vitro*. (A, B) Compound **4** inhibited the migration of HepG2 cells in a dose-dependent manner. (C, D) The invasion of HepG2 cells was observed at 24 h, and compound **4** had an inhibitory effect on the invasion of HepG2 cells. (E, F) At the end of the 24th hour, compound **4** decreased the number of pipe-like structures in HepG2 cells. (Data was represented as the means ± SD, n = 3. * $P < 0.05$, ** $P < 0.01$, *** $P < 0.001$).

Invasion and metastasis of cancer cells are the main factors of poor prognosis and easy recurrence and metastasis of cancer. Invasion and metastasis are multistep and complex process regulated by a series of genes, involving the adhesion of tumor cells, matrix degradation, tumor cell migration, tumor angiogenesis and so on (You et al., 2017, Prahl and Odde, 2018). To further study the effects of compound **4** on the invasion, migration and vasculogenic mimicry formation of liver cancer cells, we conducted wound healing, transwell and 3D culture assays with different concentrations of compound **4**. Wound healing assay results showed that compound **4** can significantly inhibit the migration ability of HepG2 cells in a dose-dependent manner (Fig. 6A, 6B). In the transwell assay, the invasion ability of the HepG2 cells was significantly inhibited by compound **4** (Fig. 6C, 6D). The 3D culture assay showed that compound **4** inhibited VM formation of HepG2 cells (Fig. 6E, 6F). These results indicates that compound **4** will be a potential drug candidate for HCC invasion, metastasis and angiogenesis.

*3.3. Compound **4** inhibits the invasion and metastasis of HepG2 cells by inhibiting EMT*

Metastasis of hepatocellular carcinoma consists of multiple processes, including EMT, characterized by loss of epithelioid features and gain of mesenchymal properties (Babaei et al., 2021). Epithelial-mesenchymal transformation (EMT) is considered a mechanism leading to tumor metastasis, and E-cadherin, Snail1, N-cadherin and Vimentin are known as EMT markers. E-cadherin is one of the epithelial markers, while Snail1, N-cadherin and Vimentin are mesenchymal markers (Loh et al., 2019). Recently, several articles have been demonstrated the EMT involvement in cancer progression and in metastasis formation, underlining that EMT is a significant event for triggering metastatic process (Smith and Bhowmick, 2016). In tumor cells with epithelial-mesenchymal transition, E-cadherin expression was decreased and N-cadherin, Vimentin and Snail1 expression were increased. In order to further determine whether compound **4** inhibited the invasion and migration of HCC cells by inhibiting EMT, we detected the expression of EMT markers in HepG2 cells by western blotting method. Western blotting results showed that compound **4** inhibited the expression of Snail1, N-cadherin and Vimentin in a dose-dependent manner. The expression levels of E-cadherin were increased by compound **4** (Fig. 7A, 7B). The results showed that compound **4** can inhibits the EMT process in HepG2 cells. Twist1, a member of the basic helix-loop-helix transcription factor family, is one of the important transcription factors that induce EMT, cell migration and invasion dur-

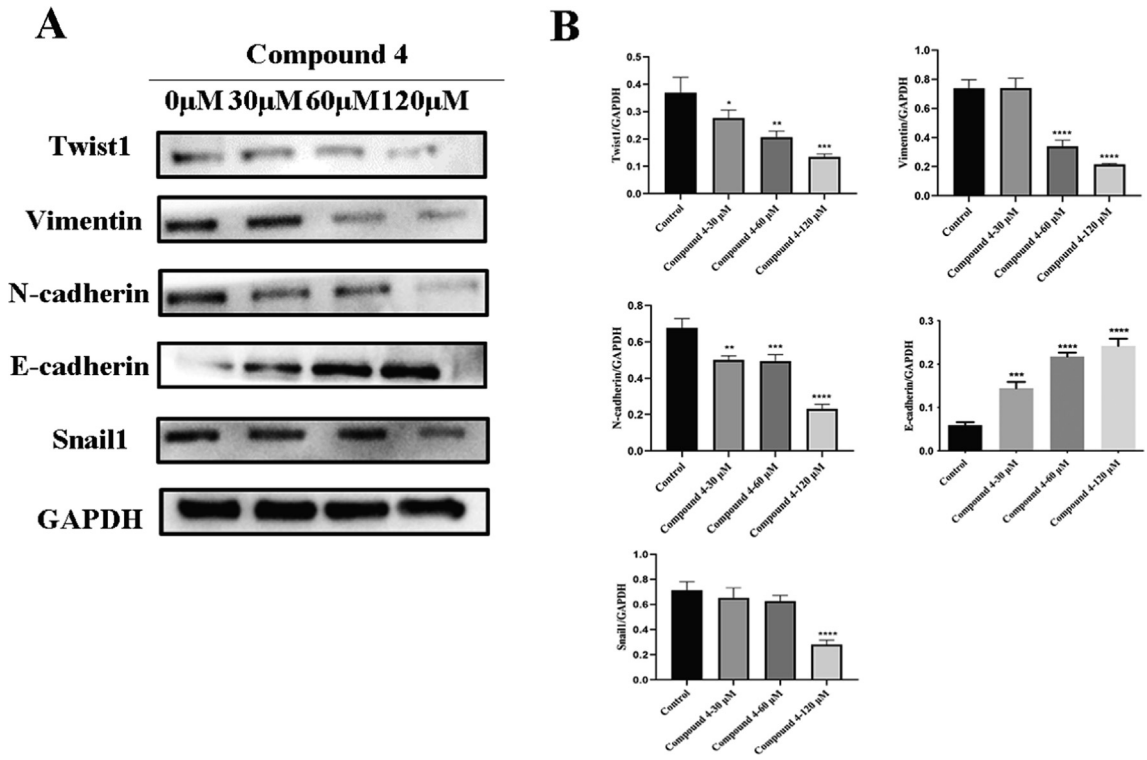

Fig. 7 Compound **4** inhibited the invasion and metastasis of HepG2 cells by inhibiting EMT. (A, B) Western blot analysis showed that E-cadherin expression was increased and Vimentin, Snail1, N-cadherin and Twist1 expression were decreased in compound **4** treated groups compared with the negative control. (Data was represented as the means ± SD, n = 3. * $P < 0.05$, ** $P < 0.01$, *** $P < 0.001$).

ing embryonic development and in cancer cells. Ectopic expression of Twist1 in Twist1-negative cancer cells is sufficient to induce EMT and cancer stem-like cell properties (Greco et al., 2021). In this study, we also evaluated the effect of compound **4** on the expression of Twist1 in HepG2 cells. The results showed that compound **4** inhibited the expression of Twist1 in a dose-dependent manner. These results indicate that compound **4** inhibits the EMT process of HCC cells by inhibiting the expression of Twist1. To our knowledge, this is the first investigation of the mechanism of the antimetastatic activity of lindenrane sesquiterpenoids. EMT plays an important role in the migration and invasion of HCC. Inhibitors targeting the EMT process will be used as adjuvant therapy for chemotherapy or targeted drugs, which can improve the clinical outcome of current cancer treatment.

4. Conclusions

Seven compounds, including one new phenylpropenol ester and three new lindenrane sesquiterpenes, were separated and elucidated from *C. japonicus*. The anti-migration potencies of all isolates were screened with HepG2 cells through the wound healing assay and compound **4** exhibited the best antimigration activity. Furthermore, compound **4** inhibited cell migration, invasion, and vasculogenic mimicry in a dose-dependent manner. The antimetastatic effect of compound **4** was associated with restraining the epithelial-mesenchymal transition in HepG2 cells by down-regulating the expression of Twist1. Compound **4** deserves further investigation as an anticancer candidate against metastatic hepatic carcinoma.

Declaration of Competing Interest

The authors declare that they have no known competing financial interests or personal relationships that could have appeared to influence the work reported in this paper.

Acknowledgements

This study was supported by the National Key Research and Development Program of China (Grant No. 2018YFA0507203), the National Natural Science Foundation of China (Grant No. 81871972), the 111 Project (Grant No. B20016), and Open fund research project of State Key Laboratory of Medicinal Chemical Biology (Nankai University) (Grant No. 2018121).

Appendix A. Supplementary data

Supplementary data to this article can be found online at https://doi.org/10.1016/j.arabjc.2022.104100.

References

Abou-Alfa, G.K., Meyer, T., Cheng, A.L., El-Khoueiry, A.B., Rimassa, L., Ryoo, B.Y., Cicin, I., Merle, P., Chen, Y., Park, J. W., Blanc, J.F., Bolondi, L., Klümpen, H.J., Chan, S.L., Zagonel, V., Pressiani, T., Ryu, M.H., Venook, A.P., Hessel, C., Borgman-Hagey, A.E., Schwab, G., Kelley, R.K., 2018. Cabozantinib in

patients with advanced and progressing hepatocellular carcinoma. N. Engl. J. Med. 379, 54–63.
Babaei, G., Aziz, S.G., Jaghi, N.Z.Z., 2021. EMT, cancer stem cells and autophagy; The three main axes of metastasis. Biomed. Pharmacother. 133, 110909.
Braun, F., Schäfer, J.P., Dobbermann, H., Becker, T., Linecker, M., 2022. Hepatocellular carcinoma. Chirurgie (Heidelb) 93, 635–643.
Bruix, J., Qin, S., Merle, P., Granito, A., Huang, Y.H., Bodoky, G., Pracht, M., Yokosuka, O., Rosmorduc, O., Breder, V., Gerolami, R., Masi, G., Ross, P.J., Song, T., Bronowicki, J.P., Ollivier-Hourmand, I., Kudo, M., Cheng, A.L., Llovet, J.M., Finn, R.S., LeBerre, M.A., Baumhauer, A., Meinhardt, G., Han, G., RESORCE Investigators, 2017. Regorafenib for patients with hepatocellular carcinoma who progressed on sorafenib treatment (RESORCE): a randomised, double-blind, placebo-controlled, phase 3 trial. Lancet 389, 56–66.
Chi, J., Wei, S., Gao, H., Xu, D., Zhang, L., Yang, L., Xu, W., Luo, J., Kong, L., 2019. Diverse chemosensitizing 8, 9-secolindenane-type sesquiterpenoid oligomers and monomers from *Sarcandra glabra*. J. Org. Chem. 84, 9117–9126.
D'Ambrosio, M., Ciocarlan, A., Colombo, E., Guerriero, A., Pizza, C., Sangiovanni, E., Dell'Agli, M., 2015. Structure and cytotoxic activity of sesquiterpene glycoside esters from *Calendula officinalis* L.: studies on the conformation of viridiflorol. Phytochemistry 117, 1–9.
Ding, Y., Wang, T., Chen, T., Xie, C., Zhang, Q., 2020. Sesquiterpenoids isolated from the flower of *Inula japonica* as potential antitumor leads for intervention of paclitaxel-resistant non-small-cell lung cancer. Bioorg. Chem. 101, 103973.
Fan, X., Zi, J., Zhu, C., Xu, W., Cheng, W., Yang, S., Guo, Y., Shi, J., 2009. Chemical constituents of *Heteroplexis micocephala*. J. Nat. Prod. 72, 1184–1190.
Gan, L.S., Zheng, Y.L., Mo, J.X., Liu, X., Li, X.H., Zhou, C.X., 2009. Sesquiterpene lactones from the root tubers of *Lindera aggregata*. J. Nat. Prod. 72, 1497–1501.
Greco, L., Rubbino, F., Morelli, A., Gaiani, F., Grizzi, F., de'Angelis, G.L., Malesci, A., Laghi, L., 2021. Epithelial to mesenchymal transition: a challenging playground for translational research. Current models and focus on TWIST1 relevance and gastrointestinal cancers. Int. J. Mol. Sci. 22, 11469.
Gundamaraju, R., Lu, W., Paul, M.K., Jha, N.K., Gupta, P.K., Ojha, S., Chattopadhyay, I., Rao, P.V., Ghavami, S., 2022. Autophagy and EMT in cancer and metastasis: Who controls whom? Biochim. Biophys. Acta, Mol. Basis Dis. 1868, 166431.
Huang, Z., Zhang, Z., Zhou, C., Liu, L., Huang, C., 2022. Epithelial-mesenchymal transition: the history, regulatory mechanism, and cancer therapeutic opportunities. MedComm. 3, e144.
Kawabata, J., Tahara, S., Mizutani, J., 2014. Isolation and structural elucidation of four sesquiterpenes from *Chloranthus japonicus* (Chloranthaceae). Agri. Biol. Chem. 45, 1447–1453.
Kim, S.Y., Nagashima, H., Tanaka, N., Kashiwada, Y., Kobayashi, J., Kojoma, M., 2016. Hitorins A and B, hexacyclic C(25) terpenoids from *Chloranthus japonicus*. Org. Lett. 18, 5420–5423.
Kouno, I., Hirai, A., Fukushige, A., Jiang, Z.H., Tanaka, T., 2001. New eudesmane sesquiterpenes from the root of *Lindera strychnifolia*. J. Nat. Prod. 64, 286–288.
Kudo, M., Finn, R.S., Qin, S., Han, K.H., Ikeda, K., Piscaglia, F., Baron, A., Park, J.W., Han, G., Jassem, J., Blanc, J.F., Vogel, A., Komov, D., Evans, T.R.J., Lopez, C., Dutcus, C., Guo, M., Saito, K., Kraljevic, S., Tamai, T., Ren, M., Cheng, A.L., 2018. Lenvatinib versus sorafenib in first-line treatment of patients with unresectable hepatocellular carcinoma: a randomised phase 3 non-inferiority trial. Lancet 391, 1163–1173.
Lee, C., Cheung, S.T., 2019. STAT3: An emerging therapeutic target for hepatocellular carcinoma. Cancers (Basel) 11, 1646.
Liu, Q., Ahn, J.H., Kim, S.B., Lee, C., Hwang, B.Y., Lee, M.K., 2013. Sesquiterpene lactones from the roots of *Lindera strychnifolia*. Phytochemistry 87, 112–118.
Loh, C.Y., Chai, J.Y., Tang, T.F., Wong, W.F., Sethi, G., Shanmugam, M.K., Chong, P.P., Looi, C.Y., 2019. The E-cadherin and N-cadherin switch in epithelial-to-mesenchymal transition: signaling, therapeutic implications, and challenges. Cells 8, 1118.
Nanjing University of Chinese Medicine, 2006. Dictionary of Chinese Traditional Medicine (Zhong Yao Da Ci Dian). Shanghai Science and Technology Press, Shanghai.
Prahl, L.S., Odde, D.J., 2018. Modeling cell migration mechanics. Adv. Exp. Med. Biol. 1092, 159–187.
Smith, B.N., Bhowmick, N.A., 2016. Role of EMT in metastasis and therapy resistance. J. Clin. Med. 5, 17.
Sumioka, H., Harinantenaina, L., Matsunami, K., Otsuka, H., Kawahata, M., Yamaguchi, K., 2011. Linderolides A-F, eudesmane-type sesquiterpene lactones and linderoline, a germacrane-type sesquiterpene from the roots of *Lindera strychnifolia* and their inhibitory activity on NO production in RAW 264.7 cells in vitro. Phytochemistry 72, 2165–2171.
Sun, Z.-H., Tan, N.-H., Zeng, G.-Z., Zhang, Y.-M., 2016. Two new cinnamyl isovalerate derivatives from *Sabina gaussenii*. Molecules 21, 571.
Tella, S.H., Kommalapati, A., Mahipal, A., Jin, Z., 2022. First-line targeted therapy for hepatocellular carcinoma: role of atezolizumab/bevacizumab combination. Biomedicines 10, 1304.
Thu Huong, T., Van Thong, N., Thi Minh, T., Huyen Tram, L., Tuan Anh, N., Duc Cuong, H., Van Cuong, P., Ca, V., D.,, 2014. Chloranerectuslactone V, a new sesquiterpene from *Chloranthus erectus* verdc. Lett. Org. Chem. 11, 639–642.
Xie, C., Sun, L., Liao, K., Liu, S., Wang, M., Xu, J., Bartlam, M., Guo, Y., 2015. Bioactive *ent*-pimarane and *ent*-abietane diterpenoids from the whole plants of *Chloranthus henryi*. J. Nat. Prod. 78, 2800–2807.
Yan, H., Ba, M.Y., Li, X.H., Guo, J.M., Qin, X.J., He, L., Zhang, Z. Q., Guo, Y., Liu, H.Y., 2016. Lindenane sesquiterpenoid dimers from *Chloranthus japonicus* inhibit HIV-1 and HCV replication. Fitoterapia 115, 64–68.
Yan, H., Li, X.-H., Zheng, X.-F., Sun, C.-L., Liu, H.-Y., 2013. Chlojaponilactones B-E, four new lindenane sesquiterpenoid lactones from *Chloranthus japonicus*. Helv. Chim. Acta 96, 1386–1391.
You, K., Sun, P., Yue, Z., Li, J., Xiong, W., Wang, J., 2017. NOR1 promotes hepatocellular carcinoma cell proliferation and migration through modulating the Notch signaling pathway. Exp. Cell Res. 352, 375–381.
Zhao, J.J., Guo, Y.Q., Yang, D.P., Xue, X., Liu, Q., Zhu, L.P., Yin, S., Zhao, Z.M., 2016. Chlojaponilactone B from Chloranthus japonicus: suppression of inflammatory responses via inhibition of the NF-kappa B signaling pathway. J. Nat. Prod. 79, 2257–2263.
Zhang, C.F., Nakamura, N., Tewtrakul, S., Hattori, M., Sun, Q.S., Wang, Z.T., Fujiwara, T., 2002. Sesquiterpenes and alkaloids from *Lindera chunii* and their inhibitory activities against HIV-1 integrase. Chem Pharm Bull (Tokyo) 50, 1195–1200.
Zhang, M., Wang, J.S., Wang, P.R., Oyama, M., Luo, J., Ito, T., Iinuma, M., Kong, L.Y., 2012. Sesquiterpenes from the aerial part of *Chloranthus japonicus* and their cytotoxicities. Fitoterapia 83, 1604–1609.
Zheng, N., Zhang, S., Wu, W., Zhang, N., Wang, J., 2021. Regulatory mechanisms and therapeutic targeting of vasculogenic mimicry in hepatocellular carcinoma. Pharmacol. Res. 166, 105507.
Zhuo, Z.G., Wu, G.Z., Fang, X., Tian, X.H., Dong, H.Y., Xu, X.K., Li, H.L., Xie, N., Zhang, W.D., Shen, Y.H., 2017. Chlorajaponols A-F, sesquiterpenoids from *Chloranthus japonicus* and their in vitro anti-inflammatory and anti-tumor activities. Fitoterapia 119, 90–99.